Volume 18, Number 5, 2025. pp. 613-628

Jordan Journal of Physics

ARTICLE

Semi-Empirical D-L Correlation for Profiling and Parameterizing Alpha Particle Tracks in Nuclear Detector CR-39 at Various Etching Temperatures

Saeed Hassan Saeed[a] and **Abrar Qasim Al-Ramadhani**[b]

[a] *Department of Cosmetic Techniques and Laser, Al-Hadba University-College of Health and Medical Techniques, Mosul, Iraq.*

[b] *Education Directorate of Kirkuk, Iraq.*

Doi: **https://doi.org/10.47011/18.5.5**

Received on: 10/08/2024; *Accepted on: 27/02/2025*

Abstract: Imaging track profiles and directly measuring their lengths is more challenging than imaging and measuring their diameters. This paper focuses on determining alpha-particle track profiles and lengths in the CR39 nuclear detector by utilizing the track's diameter-length (D-L) correlation to obtain actual track lengths from direct measurements of track diameters. Alpha particles with energies ranging from 3.5 to 5.3 MeV were used to irradiate the detector, which was then etched with a 6.25N NaOH solution at varying temperatures. The track parameters, such as the experimental bulk etch rate (VB), alpha energies, etching temperatures, and etching times, were input into the Track-Test program to calculate theoretical track lengths and create D-L calibration curves based on the Green *et al.* equation. The measured track diameters were projected onto curves to extract semi-empirical track lengths (L), track depth (x), etch rate (VT), etch rate ratio (V), and residual range (R'). MATLAB was used to plot the relationship between V and R', enabling the determination of optimal V(R') curves and new coefficients for the Green *et al*. equation. Using these newly derived coefficients, the Track-Test program applied the Green et al. equation to determine the profiles and evolution stages of the tracks. The D–L correlation method yielded track lengths and associated parameters that were consistent with direct microscopic measurements. This approach offers a viable, efficient, and straightforward alternative to direct imaging of longitudinal track profiles, which often demands considerable time, effort, and specialized techniques. Overall, the D–L correlation method provides reliable results comparable to those obtained from direct track-length measurements and thus represents a valuable tool for determining actual track lengths in nuclear detector applications.

Keywords: Track profiles, CR-39 detector, Etching temperature, Etching rates, Track depth, Track-Test.

1. Introduction

Solid-state nuclear track detectors (SSNTDs) are recognized as reliable tools for identifying the tracks of charged particles and ions. Polyallyl diglycol carbonate (PADC) detectors, specifically the CR-39, are among the most widely used types in many scientific fields [1-4]. Measurements of track length (depth), rather than the width, have received increasing attention in recent studies on the track geometry of charged particles in SSNTDs. The use of microscopic images of etched track profiles facilitates the direct measurement of track lengths, the monitoring of the evolution of track shapes, and the subsequent determination of their parameters. Calculating the track parameters directly from microscopic images of the track lengths results in exact estimates that closely reflect how the track evolves as the etching process progresses [5-7].

Corresponding Author: Saeed Hassan Saeed **Email**: profdrsaeed@gmail.com

The lengths and depths of etched tracks in the CR-39 detector are measured and recorded using a variety of imaging techniques. One of these methods is the resin-replica technique, which employs a certain epoxy to create exact copies of the etched tracks whose heights are determined using contact stylus profilometry [8-10]. Track depths can also be obtained, along with three-dimensional imagery, using a confocal microscope [11-13]. Another approach involves selectively fracturing the etched detector along a plane perpendicular to its surface to expose lateral profiles and estimate track depths [14, 15].

In the majority of our articles [7, 16-18], the "lateral irradiation" technique of the detector is proposed, which involves irradiating the detector's sharp side rather than its surface. The longitudinal sections of the etched tracks are photographed from the detector surface with a digital camera mounted on a conventional optical microscope. The collected track photos are then analyzed, and the necessary measurements are made using a PC connected to the camera. This method is straightforward and produces good results compared to other ways, as it does not require sophisticated techniques. In addition, we have suggested a semi-empirical method (under specific initial assumptions) for determining track lengths based on direct experimental measurements of track diameters rather than profile photographs [18]. This indirect method accurately predicts track lengths and depths, residual range, track etching rates, and the profiles of etched tracks.

Several computer programs, such as TRAK-TEST, TRACK-VISION, CR39, and the TRACK-P programs, have been developed to simulate and plot the etched track profiles in the CR-39 detector in two and three dimensions, as well as to determine a number of parameters. These parameters include the major and minor diameter, length, depth, residual range, and track etching rates [16, 19-21].

The main objective of this work is to present a different semi-experimental method for determining precise lengths and plotting the profiles of etched tracks in the CR-39 detector. This method, referred to as the track's diameter-length (D-L) correlation method [22], is based on calculating the track lengths by measuring their diameters instead of measuring them directly from the experimental track photos. So, by obtaining D-L calibration curves for the alpha particle energies and etching temperatures used, we can determine the rates at which the track lengths L'(t) and other parameters change. These parameters are the track length (L), residual range (R'), and etching rates (V_T & V). Using the Track-Test program and the obtained data, we can also plot the etched-track profiles and trace their development stages.

2. Experiment

2.1. Track Diameter Measurement

A CR-39 detector slice was cut into 1 x 1cm^2 pieces and irradiated under vertical incidence with alpha particles from a radioactive ^{241}Am source (0.5 μCi) at energies of 5.3, 4.7, 4.1, and 3.5 MeV. SRIM software was used to obtain energies less than the source's primary energy of 5.485 MeV by adjusting the distance between the detector and the radioactive source [23]. An aqueous NaOH solution of molarity 6 N was used to etch the irradiated detectors at 60, 70, and 80 ± 1 °C for successive etching intervals ranging from 0.5 to 20 h. Following etching, the detectors were thoroughly cleaned with distilled water, dried, and then examined to measure the diameters of the tracks utilizing a digital camera (MDC E-5C) mounted on an optical microscope (Noval) and linked to a PC, as shown in Fig.1. This procedure was repeated for studied alpha energies and etching temperatures for the required etching times in each case.

The thickness difference approach was used to compute the bulk etching rate (V_B). Unirradiated detector pieces were etched in a 6 N NaOH for 1-10 h at temperatures of 60, 70, and 80 °C. The layer thickness peeled from the detector surface was obtained by subtracting the detector thicknesses prior to and following etching. From the plot of etching time versus removed thickness, V_B was computed as $V_B = \Delta h/\Delta t$ (μm/h) [1]. In this work, V_B was found to be 1.421 μm/h.

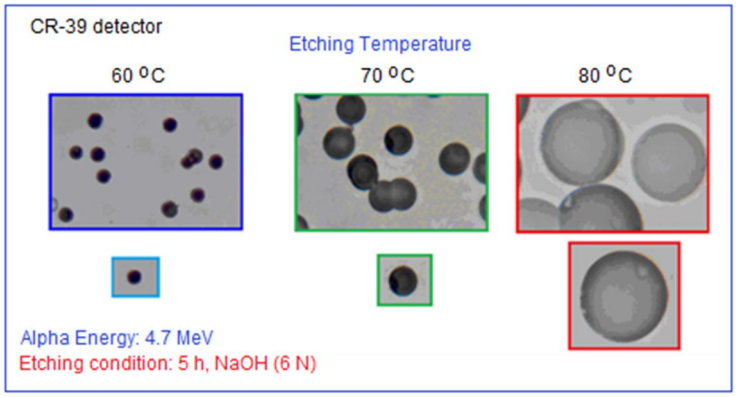

FIG. 1. Images of alpha particle track diameters at 4.7 MeV in the CR-39 detector, etched in NaOH(6N) solution for 5 hours at various temperatures.

2.2. Extracting Track Length, Profile, and Other Parameters

Instead of directly measuring the track lengths, we suggested the D-L correlation approach to infer the track lengths indirectly from experimental observations of the track diameters. By entering our experimental data into the TRACK-TEST (T-T) software [20] and using the Green *et al* (1982) formula of the etch rate ratio (V), provided in the T-T software with its default coefficients for CR-39, we can theoretically determine the profiles and lengths of the etched tracks. The entered data include alpha particle energy (E), bulk etching rate (V_B) at a given temperature (T), iterative etching times (t), and normality (N) of the chemical solution. From the generated track profiles, the track lengths and diameters are identified for each alpha energy and etching temperature over a set of selected etching periods, including the times of the experimentally measured diameters under given conditions.

The obtained D-L data set was plotted to extract the track D-L calibration curves, which were subsequently used to estimate the semi-empirical track lengths corresponding to the experimentally recorded diameters at the specified periods. By projecting the experimentally measured track diameters onto the appropriate calibration curve for each energy and etching temperature, we determine the semi-empirical lengths associated with the measured diameters for the relevant etching times, as well as for additional selected times in each case. Using these semi-empirical lengths together with the measured V_B, a number of track parameters are calculated, including the track length growth rate (dL/dt), track depth (x), residual range (R'), track etching rate (V_T), and etch rate ratio (V).

The resulting V values are plotted versus corresponding R' values for selected etching intervals and for alpha-particle energies of 5.3, 4.7, 4.1, and 3.5 MeV at etching temperatures of 60, 70, and 80 °C. To obtain optimal curve fits and updated coefficients for the V equation, the $V(R')$ data for all conditions are fitted using MATLAB in accordance with the Green et al. relation [24]. These optimized coefficients, along with the experimental inputs, are then supplied to the Track-Test program, where the Green *et al*. formula is applied again to determine the actual track profiles (longitudinal sections) in CR-39 corresponding to the experimentally measured diameters. As the etching process proceeds, the evolution of track growth and the successive development stages are also determined according to the specified alpha-particle energy, etching temperature, and etching interval.

3. Results and Discussion

3.1. Track Diameter and Its Growth Rate

The sizes of the tracks vary with the energy of the alpha particles used to irradiate the detector; higher alpha energies produce smaller track diameters. Figure 2 illustrates the change in track diameter (D) with etching period (t) for alpha particles with energies ranging from 5.3 to 3.5 MeV. The figure also shows that, for the same etching period, track diameters increase with increasing temperature of the chemical solution. Thus, the track size grows as the etching temperature rises from 60 to 80 °C.

The track diameter growth rate (V_D) is defined as the rate at which the track diameter

increases due to chemical etching of the detector exposed to charged particles. Since the track diameter varies linearly with etching time, V_D has a single value for particles incident perpendicularly on the detector surface. As a result, the created track exhibits a circular opening in the homogeneous and isotropic detector, as in the case of CR-39. The slope ($\Delta D/\Delta t$) of the lines in Fig. 2 represents the V_D values for alpha particle energies and etching temperatures used, as shown in Table 1. It is clear that V_D has a single value in each case, and this value varies depending on the alpha particle energy and etching temperature. Figure 3 shows that V_D decreases linearly with increasing alpha energy for the three chemical solution temperatures of 60, 70, and 80 °C. On the other hand, Fig. 4 shows that V_D follows a similar pattern for all alpha energies, as it increases exponentially with the temperature of the etchant under given etching circumstances.

It is well-known that raising the chemical etchant temperature enhances the energy (velocity) of the interaction of the chemical etchant molecules with the detector material. This causes more molecules to degrade in the areas that are affected by the incident particles, accelerating the growth of the track diameter. Accordingly, within the energy range and etching conditions used here, the value of V_D is larger at high etching temperatures and low alpha energies, and vice versa. This is evident from the values of V_D listed in Table 1 and in their dependence on energy and temperature as shown in Figs. 3 and 4.

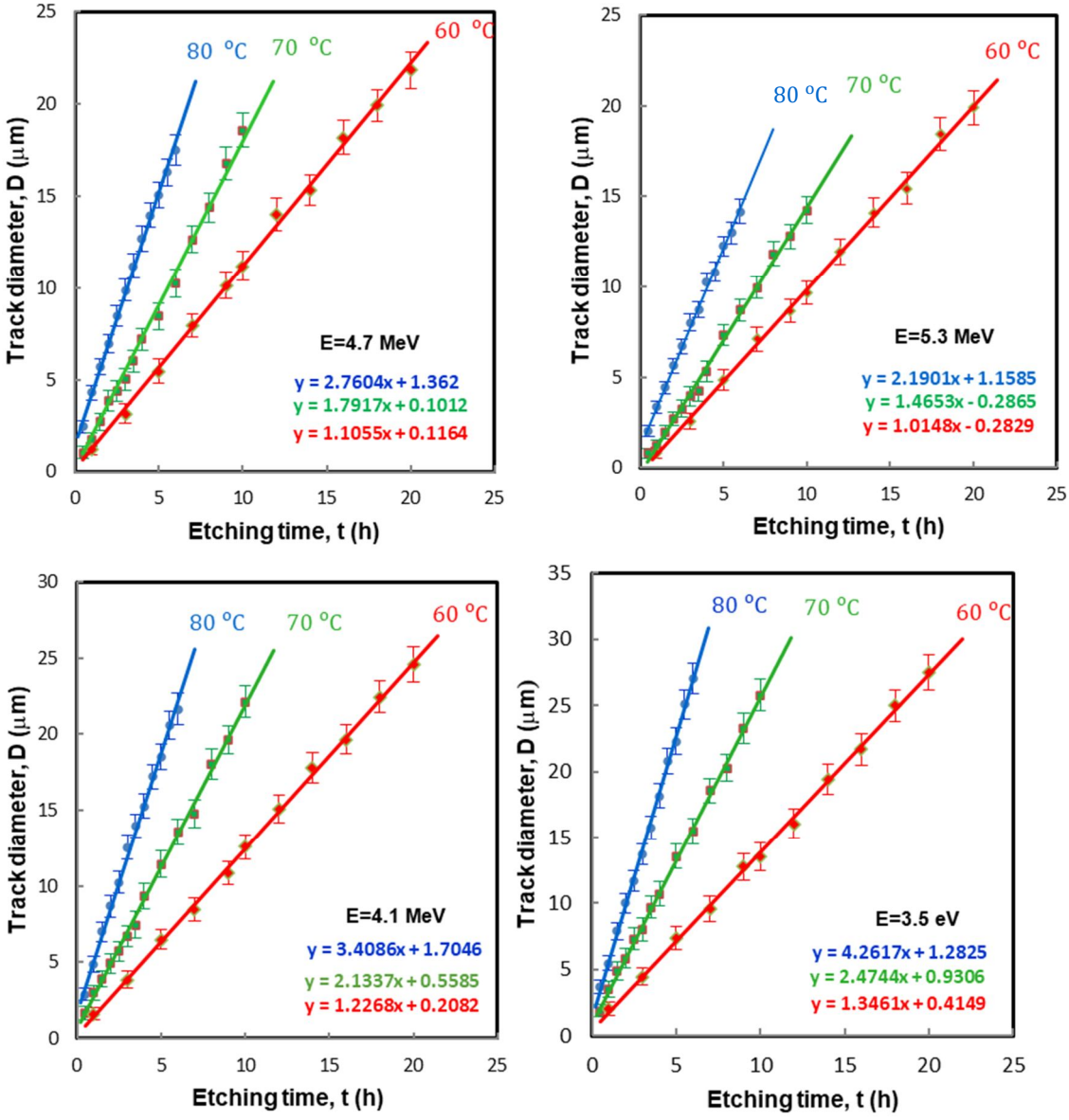

FIG. 2. Track diameter versus etching time for alpha energies of 5.3-3.5 MeV at different etching temperatures.

TABLE 1. Track diameter growth rate in CR-39 for various alpha energies and etching temperatures.

Etching Temp. (°C)	60	70	80
E (MeV)	Track diameter grow rate, V_D (µm/h)		
5.3	1.0148	1.4653	2.1901
4.7	1.1103	1.7917	2.7604
4.1	1.2268	2.1337	3.4994
3.5	1.3461	2.4744	4.2617

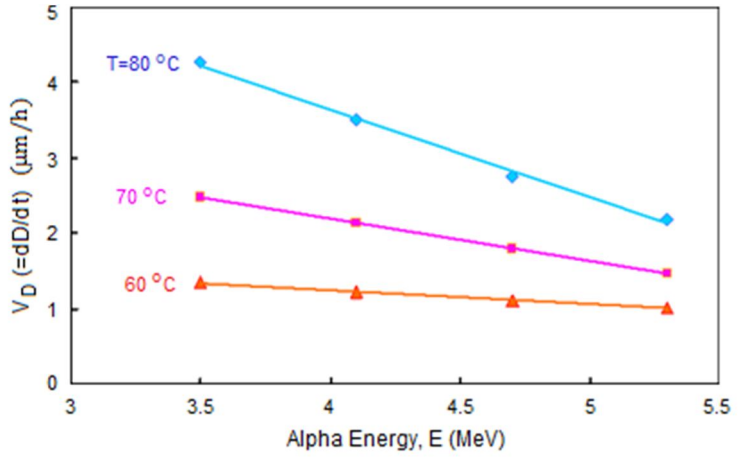

FIG. 3. Track diameter growth rate in relation to alpha energy at various etching solution temperatures.

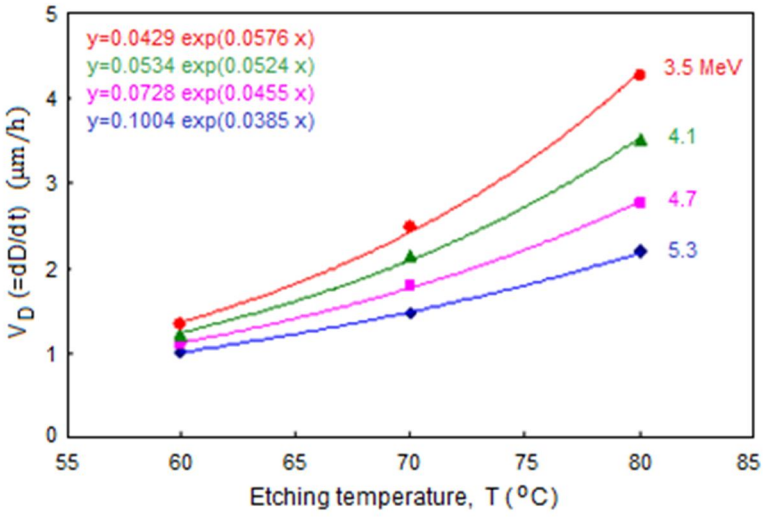

FIG. 4. Track diameter growth rate in relation to etching solution temperature for various energies of alpha particles.

3.2. Track Length

Figure 5 illustrates the change of semi-empirical track lengths with the time of etching in CR-39 for various energies and etching temperatures. The track length exhibits two distinct growth phases. In the first phase, where $V_T/V_B > 1$, the track length increases nonlinearly until it reaches a constant maximum value L_{max} at the saturation point (i.e., the start of track length saturation) [18, 25]. The track length achieves its maximum at this point when the etching extends to the end of the alpha range in the detector (the tail of the damaged path). Following this, the track length remains at its maximum saturation value (L_{max}), and the growth rate of the track length is kept at zero ($dL/dt = 0$) as the etching continues. It is also evident that the track length increases with decreasing alpha energy, corresponding to an increase in the particle's energy loss rate per unit distance in the detector. This indicates that more energy is being deposited, resulting in the rise of the energy of the damaged areas. Consequently, the etching process proceeds more quickly, enabling the removal of more damaged molecules from these regions.

The stage from the beginning of the track's appearance until the point of saturation is called the acute-cone phase. During this phase, the etched track is conical, terminating in a pointed tip located at the end of the damaged path; this structure is commonly referred to as an "etched-out" track. After saturation, the track enters the over-etching phase, during which the etchant progresses beyond the end of the damaged trajectory (i.e., beyond the alpha-particle range) into the undamaged region [12, 18]. At the beginning of this phase, the value of V_T approaches V_B, causing the pointed tip of the conical track to round off and gradually evolve into a more spherical shape as $V_T \approx V_B$.

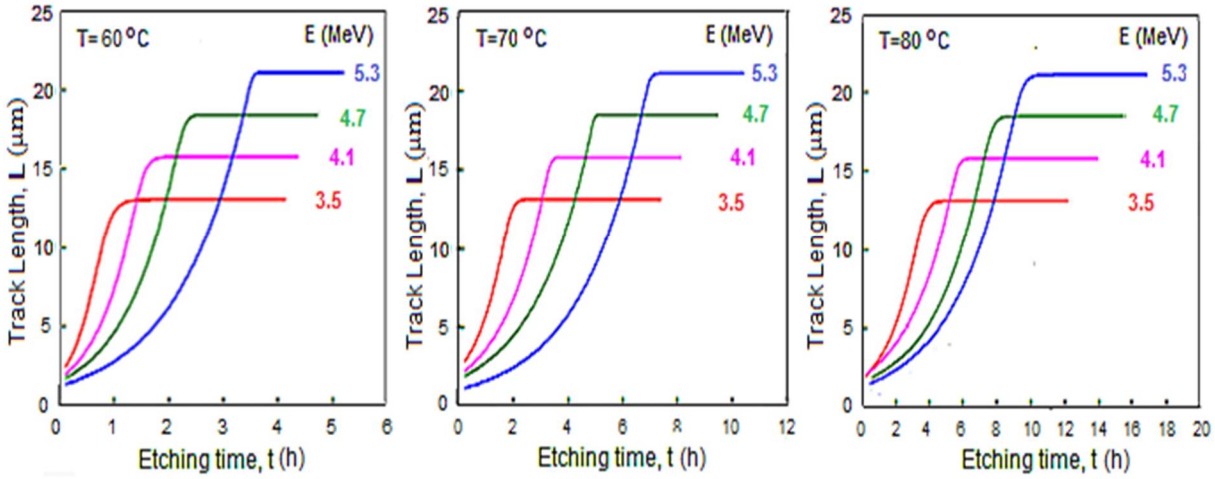

FIG. 5. Semi-empirical track lengths obtained from the D-L calibration curves versus etching time for different energies of alpha particles at etching temperatures of 60, 70, and 80 °C.

Regarding the effect of temperature on the track lengths, the graphs in Fig. 6 show that increasing the etchant temperature speeds up the degradation of the detector molecules and reduces the time required to get the same length at the same moment for the specified alpha energy. The figure also shows that, for each alpha energy, the change in track length with etching time appears as bundles corresponding to the etching temperatures 60, 70, and 80 °C at a constant concentration of etching solution. The length bundles show that the value of the maximum length (L_{max}) does not depend on the etching temperature, as it is constant in each bundle, but differs with alpha particle energy. This is evident from the leftward and downward shift of the bundles as the particle energy decreases.

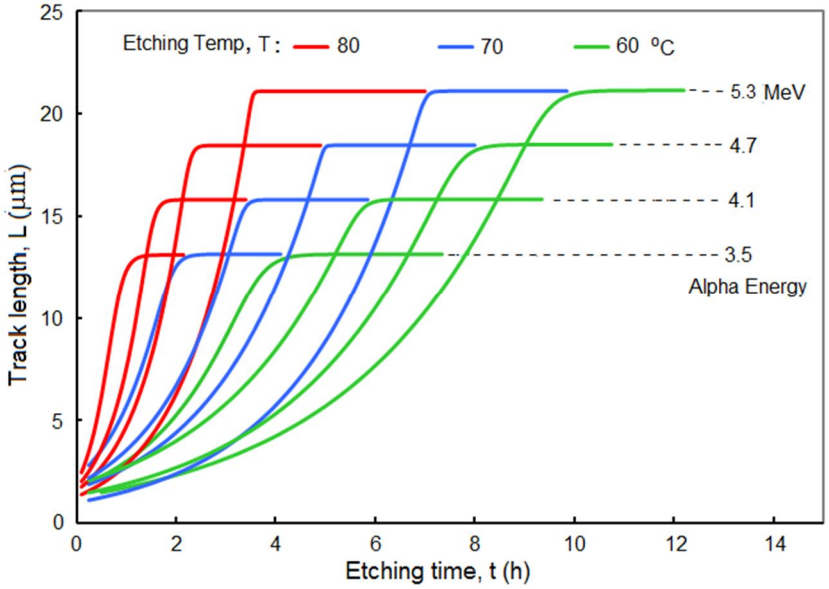

FIG. 6. Bundles of lengths against etching time for a range of alpha energies (5.3-3.5 MeV) at various etching temperatures (60, 70, and 80 °C).

3.3. Track Length Growth Rate

The track-length growth rate, denoted as $L'(t) = dL/dt$, is defined as the rate at which the track length changes over time as a result of the etching process. It is a measurement of how much material is removed from the damaged area as the etching deepens. The calculation of $L'(t)$ is important because it is related to the etching rate toward the depth of the track, V_T, which is regarded as one of the fundamental and crucial parameters in describing the track shape. Figures 7 and 8 show the change in track length growth rate with etching time and alpha particle energy, respectively.

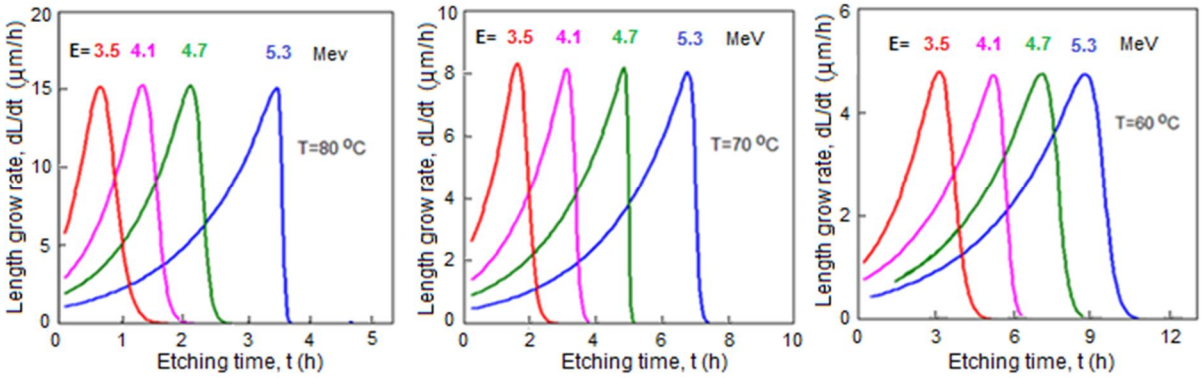

FIG. 7. Track's length growth rate versus etching time for various alpha energies at etching temperatures of 60, 70, and 80 °C.

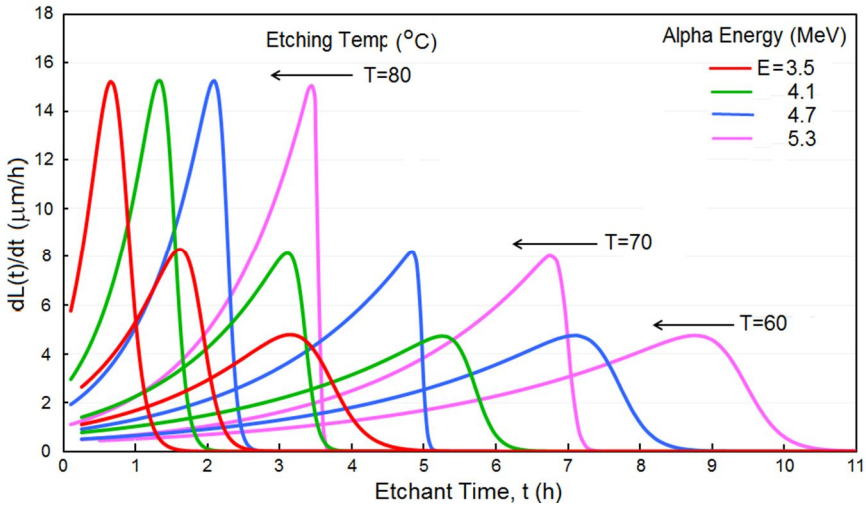

FIG. 8. Track's length growth rate versus etching time at various etching temperatures for alpha energies of 5.3-3.5 MeV.

3.4. Track Etch Rate

The track etch rate (V_T) plays an essential role in profiling the etched track. The stages of track growth, as well as the development of its length and profile, are closely connected to V_T and its variation against the etching period (t) and depth of track (x). It quantifies the velocity at which the material is eliminated from the detector along the damaged depth, which is influenced by the etching circumstances and the energy loss rate per unit distance in the detector. The V_T is calculated using the following equation [5, 26, 27]:

$$V_T = dL/dt - V_B t \quad (1)$$

Figures 9 and 10 illustrate the variation of V_T with etching time for various etching temperatures and alpha particle energies, respectively. The shape of curves is in good agreement with those recorded under different conditions [5, 7, 18].

The track depth $x(t)$ is the separation between the initial surface of the detector and the pointed head of the etched track. It is strongly correlated to V_T and can be calculated using Eq. (2) [27]:

$$x(t) = V_T(t).t\ (\mu m) \quad (2)$$

On the other hand, Eq. (3) can be used to compute the residual range $R'(t)$ [13, 20]:

$$R'(t) = R - x(t)\ (\mu m) \quad (3)$$

It is worth mentioning that there is a strong and dialectical relation between the etching rate (V_T) and the energy loss rate ($-dE/dx$), and then with the amount of damage caused in the detector by the incident particles.

The chemical etching solution attacks the damaged portions more aggressively, raising the potential energy of these areas and thereby increasing the V_T even more. As the etching process advances, V_T reaches its maximum value of V_{Tmax} just before the tip of the conical track reaches the tail of the damaged path, i.e., the alpha range in CR-39. This maximum point corresponds to the position of the Bragg peak on the stopping power curve of alpha particles in air, as illustrated in Fig. 11, where the etching rate and the number of degraded molecules are at their highest. Following that, V_T drops and begins to approach the V_B value at the damaged end as it quickly reaches equality $V_T = V_B$ (1.421 µm/h in this study) once the etchant enters the undamaged area beneath the damaged region. This is consistent with the results obtained by others using different methods [6, 7, 18].

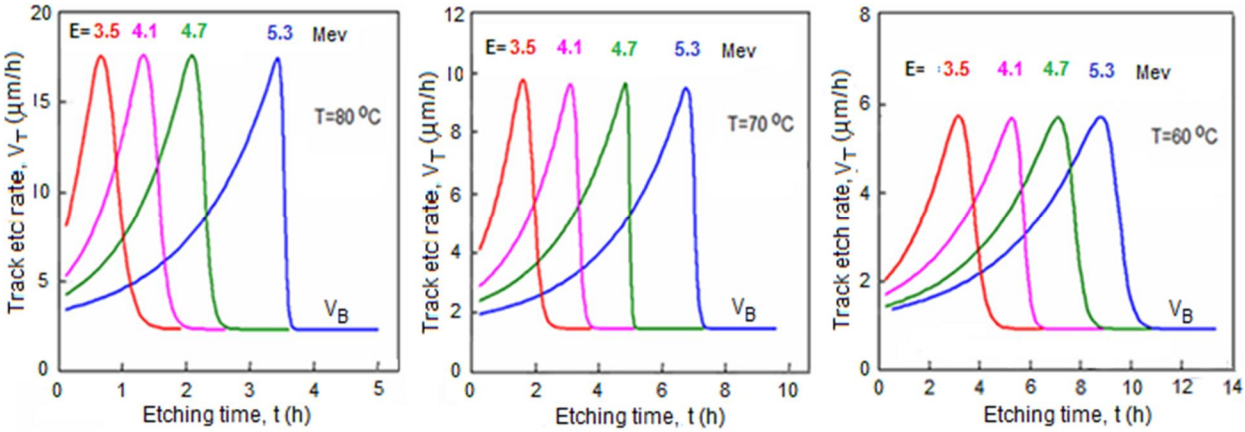

FIG. 9. Track etch rate versus etching time for various alpha energies at etching temperatures of 80, 70, and 60 °C.

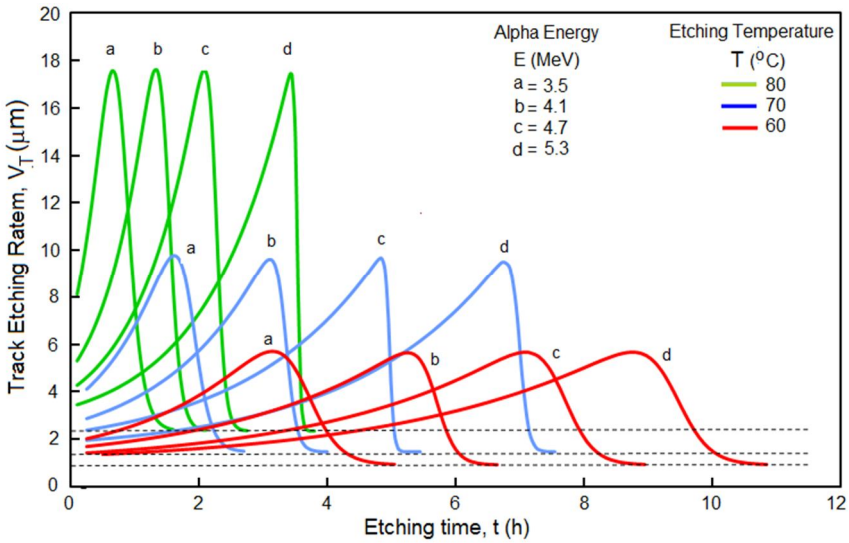

FIG. 10. Track etch rate versus etching time for alpha energies of 5.3-3.5 MeV at various etching temperatures.

3.5. Etch Rate Ratio

The etch rate ratio (V), known as the response, is another fundamental parameter describing the track, since it is related to V_T, which is an essential factor in determining the track shape evolution. For normally incident particles on the detector, V is given as [1]:

$$V = V_T / V_B \quad (4)$$

V_B is usually constant, depending on the etching conditions. Thus, the temporal pattern of V follows the same trend as V_T, differing only by a constant factor of V_B^{-1}.

Figure 11 illustrates the one-to-one correspondence among three curves: the stopping power (S) of alpha particles in air versus path length, the etch rate ratio versus track depth V(x), and the track length versus etching interval L(t). The figure highlights several key features: the residual range R', the maximum etch rate V_m, the maximum track-length growth rate $(dL/dt)_{max}$ corresponding to the Bragg peak, the saturation time t_{sat}, the maximum track length L_{max} at the end of the alpha range or damaged trajectory, and the behavior of other parameters related to track-profile development throughout both stages of track growth.

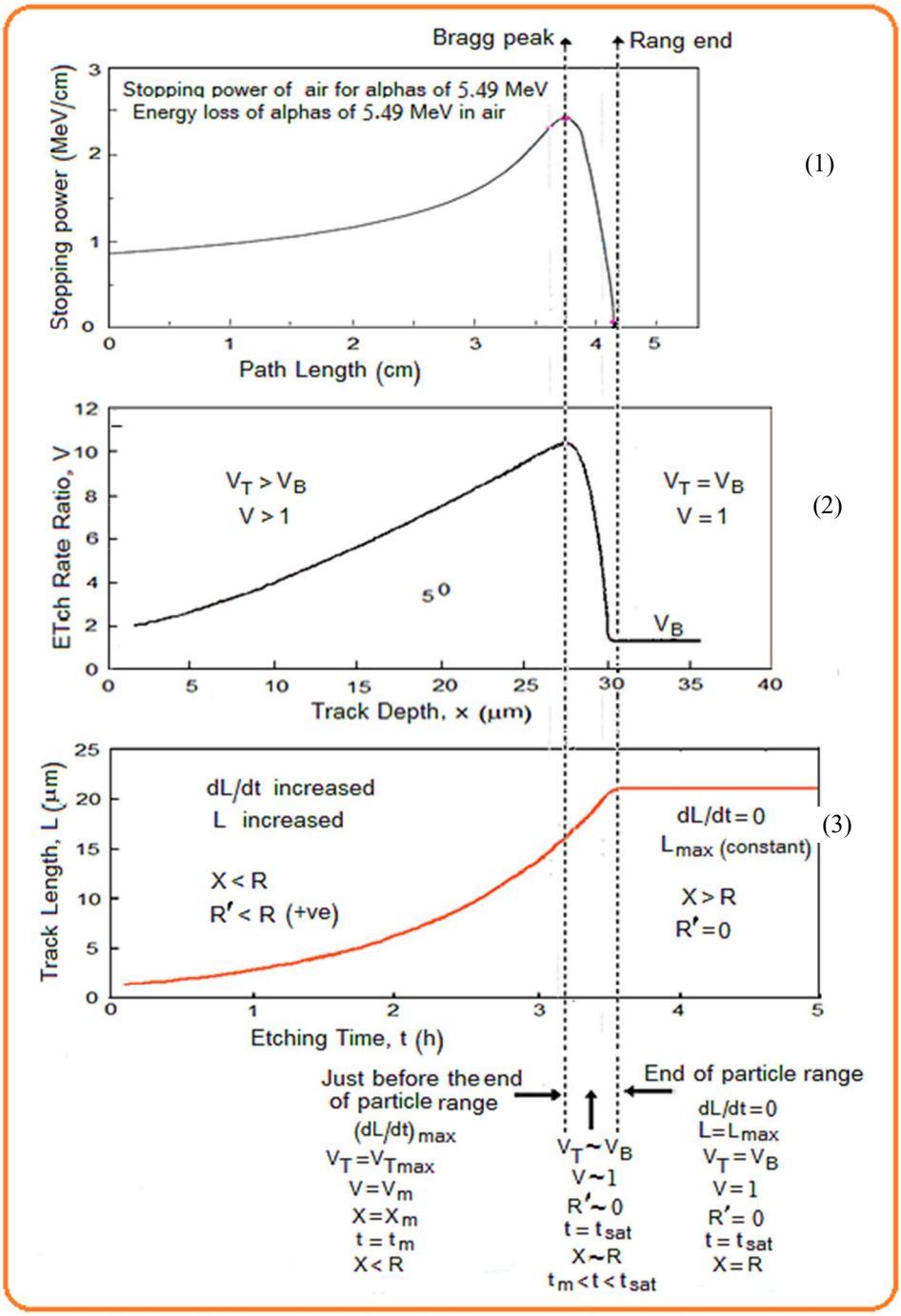

(1) https://en.wikipedia.org/wiki/Bragg_peak Wagenaar, Douglas (1995). "7.1.3 The Bragg Curve". *Radiation Physics Principles.* (2) & (3) The present work.

FIG. 11. Coincidence among three curves: the stopping power of alpha particles in air, the etch rate ratio versus track depth, and the track length versus etching interval.

3.6. Etch Rate Ratio and Residual Range

One of the crucial steps in analyzing the track profiles and drawing them in accordance with the measured experimental data is the determination of etching rates, particularly the V_T and V, and plotting them with respect to R′. Several researchers presented and used a number of computer programs to theoretically sketch the profile of the track and compute its parameters for protons and alpha particles in CR-39 and LR115 detectors [16, 19-21]. These programs are based on specific mathematical formulae for V(R′), as proposed by various researchers [7, 8, 24, 28, 29].

Figure 12 shows that the V function initially increases as the residual range (R′) increases, reaching its maximum value, $V_m(R')$, where R′ becomes very small at the point corresponding to the Bragg peak. This happens shortly before the etching reaches the limit of particle range. Once the chemical etchant reaches the damaged tail, V rapidly decreases after a short etching interval. At the same time, the track length reaches the beginning of saturation and attains a constant maximum value (L_{max}). At this point, the residual range becomes zero ($R' = 0$), the track depth equals the particle's range ($x = R$), the value of V is getting close to one ($V \approx 1$), and $V_T \approx V_B$. This shows that the conical etched track tip has arrived at the damaged tail at the alpha range end, where the track is completely etched and is referred to as the "out-etched" track. More prolonged etching times result in non-directional (scalar) etching that moves at the same rate of $V_T = V_B$ $(i.e., V = 1)$ in all directions within the undamaged area beneath the damaged path. In this case, the track is known as an "etching pit" [18, 20].

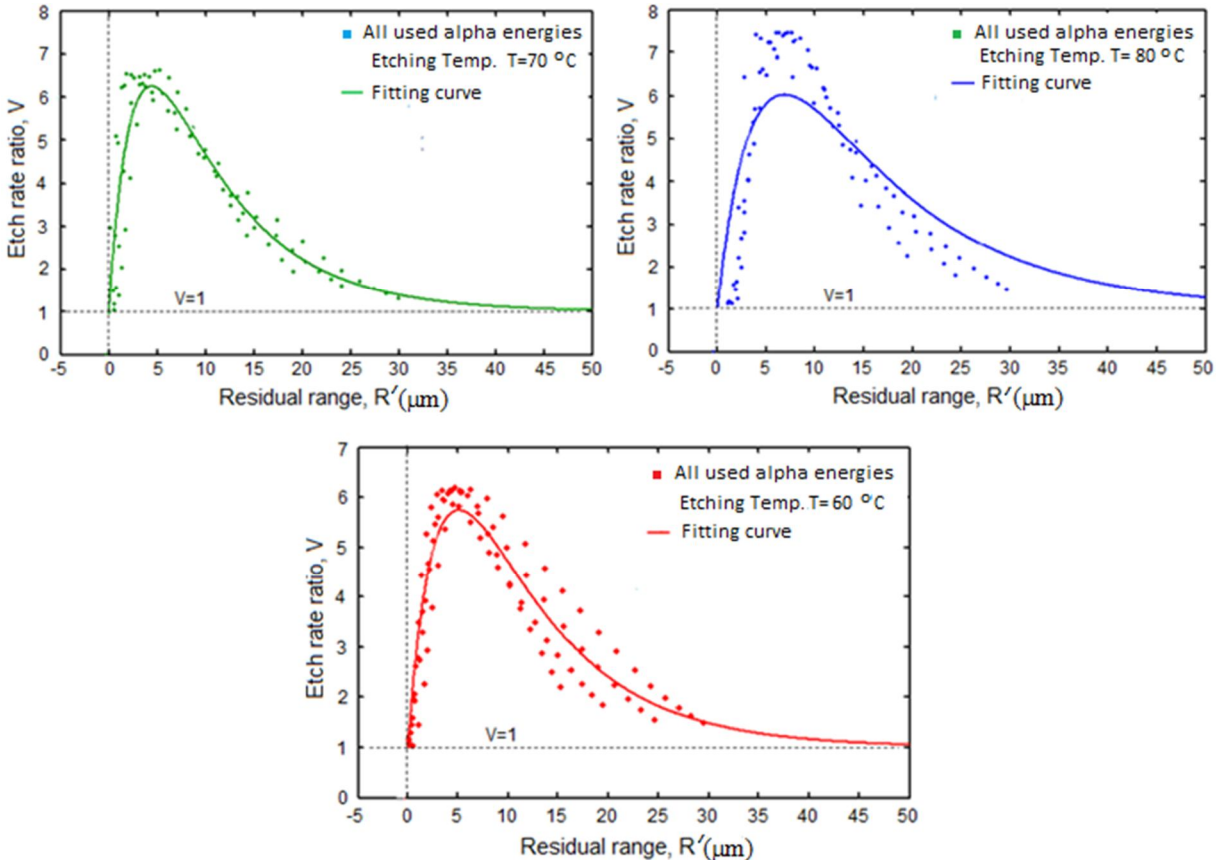

Fig. 12. The fit curves of V(R′) obtained using combined data from all alpha-particle energies for each etching temperature separately, according to the Green *et al.* (1982) formula.

3.7. Fit Curve of Etch Rate Ratio and the Coefficients

Since the etch rate ratio (V) does not vary significantly with alpha-particle energy, as shown in Fig. 12, and because it is directly related to the track depth (x) in the detector, it can be fitted as a function of the residual range. The resulting fitted curves are represented by the solid lines in the figure. By incorporating the newly obtained fitting coefficients into the Track-Test program [20], the theoretical profiles of etched tracks can be determined, and their

evolution can be traced for the investigated alpha-particle energies at the examined etching temperatures. The curve fitting between V and R' was performed using MATLAB software, based on the Green *et al.* equation [24], given by

$$V = 1 + [A_1 \exp(-B_1 R') + A_2 \exp(-B_2 R')][1 - \exp(-B_3 R')] \quad (5)$$

where $A_1, A_2, B_1, B_2,$ and B_3 are the formula's coefficients, and R' is the residual range.

The solid curves in Fig. 12 represent the optimal fits of $V(R')$ for various alpha-particle energies at each etching temperature considered individually. In contrast, Fig. 13 presents the optimal fit of the $V(R')$ function obtained by combining all alpha-particle energies and all etching temperatures simultaneously. The coefficients $A_1, A_2, B_1, B_2,$ and B_3, as well as $V_m(R')$ and R' corresponding to the maximum values, were identified from the fitting process based on our experimental data and the used etching conditions. It was found that the average values of the coefficients $A_1, A_2, B_1, B_2,$ and B_3, obtained by fitting the $V(R')$ values for all alpha energies (5.3, 4.7, 4.1, and 3.5 MeV) and all etching temperatures (60, 70, and 80 °C) simultaneously, are very close to those obtained by fitting the $V(R')$ data for all alpha-particle energies combined at each etching temperature separately. This agreement is evident from Figs. 12 and 13 and the values listed in Table 2.

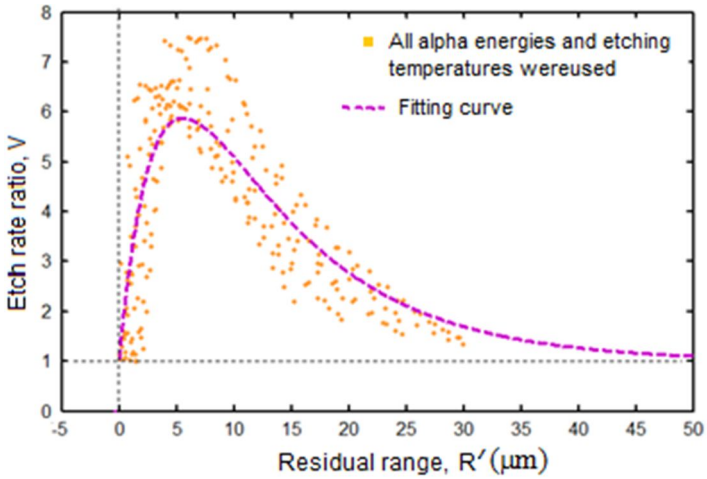

FIG. 13. Optimal fit curve of $V(R')$ obtained using combined data for all alpha-particle energies and etching temperatures, according to the Green *et al.* (1982) formula.

TABLE 2. The new coefficients of the Green *et al.* formula for V, the maximum V_m values, and the corresponding residual range (R'), for various alpha energies and etching temperatures.

Coffiecients and Parameters	Using optimal fit of V(R') values for all alpha energies together at once for each etching temperature separately				Using optimal fit of V(R') values for all alpha energies and etching temperatures together at once
	Etching Temperature °C				
	60	70	80	Average	
A_1	6.18	6.233	6.158	6.1903	6.207
A_2	6.181	5.925	5.998	6.0347	5.997
$B_1(\mu m^{-1})$	0.1079	0.1132	0.0759	0.0990	0.0948
$B_2(\mu m^{-1})$	0.1083	0.1141	0.0760	0.0995	0.0948
$B_3(\mu m^{-1})$	0.2149	0.2819	0.1731	0.2233	0.2039
V_m	5.716	6.29	6.043	6.016	5.92
R' (μm)	5.193	4.487	6.784	5.488	5.556

This indicates that the values of V are nearly independent of both the etching temperature and the alpha-particle energy to which the detector was exposed. Therefore, the $V(R')$ data for all alpha energies and etching temperatures were fitted collectively using the formula proposed in the present study. The coefficients $A_1, A_2, B_1, B_2,$ and B_3 extracted from the optimal fit were subsequently implemented in the Track-Test program,

together with other experimental parameters, to generate the alpha-particle track profiles (longitudinal sections) in CR-39. These parameters include the etching time, alpha-particle energy, and the bulk etching rate corresponding to each etching temperature. As shown in Table 2, the maximum values V_m obtained from both fitting approaches are nearly identical. This confirms the validity of performing a unified fit using the combined V data for all alpha energies and etching temperatures to determine the coefficients employed in generating track shapes and parameters that are consistent with our experimental data.

The shape and behavior of the graph representing the optimal etching rate function V(R') is consistent with the findings of Nikezic and Yu [30], who measured the track lengths directly from the track profile images for various alpha particle energies and etching conditions, as shown in Fig. 14(a). Furthermore, the behavior of the current V(R') function graph based on the D-L approach also agrees with that shown by Younis [22], who utilized the D-L approach to determine the track lengths indirectly from direct measurements of the track diameters, as shown in Fig. 14(b). He selected alpha energies of 4.4, 3.6, 2.8, and 2.0 MeV and used the etchant NaOH at 70 °C and molarities of 4, 5, 6, and 7 N, while the present study utilized alpha particles with energies of 5.3, 4.7, 4.1, and 3.5 MeV and NaOH as an etchant of molarity 6 N, where the etching was conducted at different temperatures of 80, 70, and 60 °C.

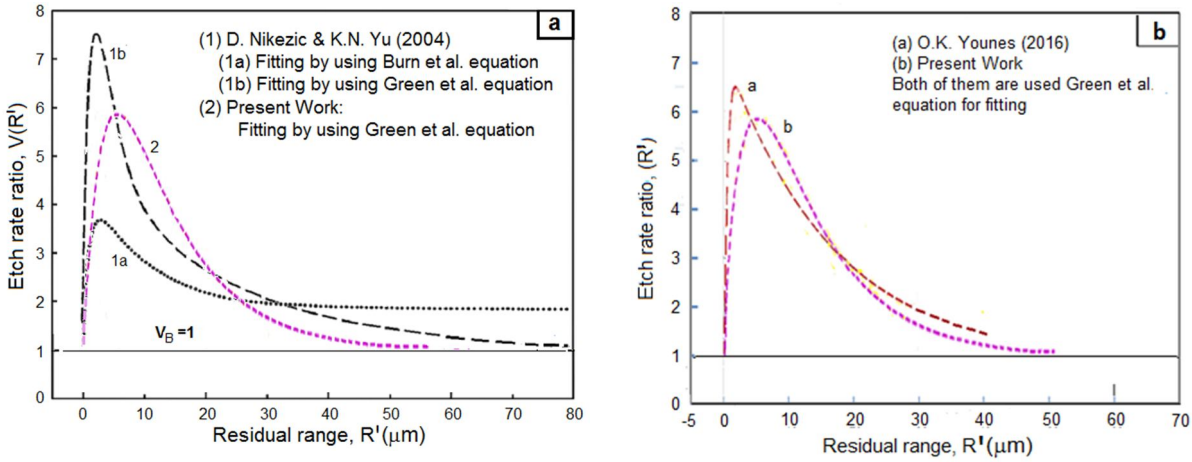

FIG. 14. Comparison of the V(R') function obtained in the present study with those reported by Nikezić and Yu [30] and Younis [22] for various alpha-particle energies and etching conditions.

3.8. Track Profiles Optimal Fit Curve of Alpha Particles Tracks in CR-39

The track profiles (longitudinal sections) and their associated parameters in the CR-39 detector were theoretically obtained by inputting the coefficients derived from the optimal fit of the V(R') curve, together with the experimental data from the present study, into the Track-Test program using the Green *et al.* equation. As inferred from the path-length behavior in Fig. 5 and illustrated in Fig. 15, the formation of track profiles during the etching process occurs in two distinct phases: the acute-cone phase within the damaged region and the over-etched phase in the intact material beneath the damaged path, beyond the alpha-particle range in the detector. As an example, Fig. 15 shows the simulated profiles of 4.7 MeV alpha-particle tracks in CR-39, together with the corresponding growth phases, track diameters, and lengths, as determined using the Track-Test software based on our experimental data. The input parameters used for this simulation are as follows: alpha-particle energy $E = 4.7$ MeV; particle incident angle $\theta = 90^{o}$; etching molarity and temperature $N = 6$, $T = 70\,^{o}C$; etching time $t = 1-10$ h; bulk etch rate $V_B = 1.421\ \mu m/h$; and the coefficients listed in Table 2, namely $A_1 = 6.207$, $A_2 = 5.997$, $B_1 = 0.09481\ \mu m^{-1}$, $B_2 = 0.09481\ \mu m^{-1}$, $B_3 = 0.2039\ \mu m^{-1}$, as applied in the Green *et al.* function given in Eq. (5)

Similar results can be obtained for the other alpha-particle energies investigated in this work (5.3, 4.1, and 3.5 MeV) and for etching temperatures of 60, 70, and 80 °C.

Acute -cone stage (sharp-track phase)						
L – changes with etching time					saturation point "*etched-out track*"	
	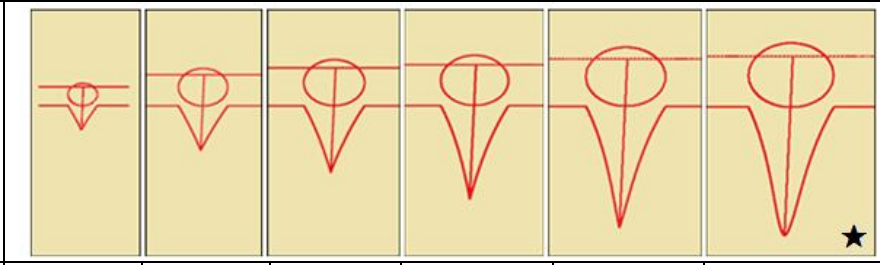					
t (h)	1.5	2	3	4	4.5	**5** = t_{sat}
L (μm)	2.852	4.175	7.806	13.644	17.043	18.544 = L_{max}
D (μm)	2.631	3.352	5.387	7.297	8.275	9.273
Over-etched Stage (spherical- track phase)						
L is approximately constant = L_{max}, & $dL/dt = 0$						
	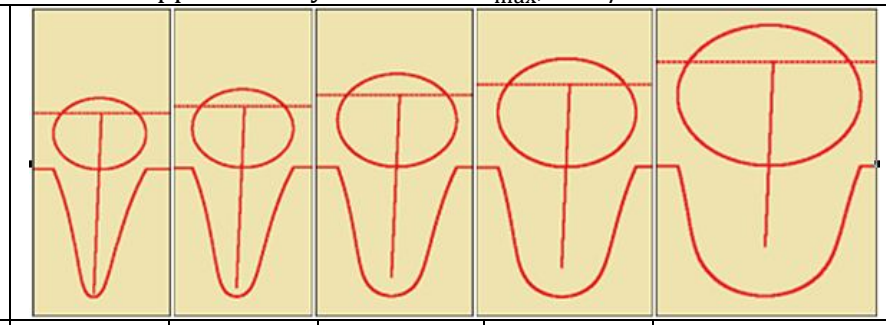					
t (h)	5.5	6	7	8	10	
L (μm)	18.544	18.571	18.571	18.571	18.571	
D (μm)	10.275	11.299	13.391	15.544	20.023	

FIG. 15. Profiles or longitudinal sections of 4.7 MeV alpha particle tracks in CR-39 under etching conditions of NaOH (6 N) at 70 °C, using the Track-Test software.

Table 3 and Fig.16 show the maximum lengths (L_{max}) of the alpha tracks in CR-39 with energies of 5.3-3.5 MeV and etching temperatures of 60, 70, and 80 °C. These values were obtained from the theoretical track profiles generated by the Track-Test software using the optimal values of A_1, A_2, B_1, B_2, and B_3 obtained from fitting the V(R') curve, given in Table 2.

TABLE 3. Comparison of maximum track lengths in CR-39 for various alpha-particle energies at all etching temperatures, obtained theoretically using the Track-Test software with the new coefficients from the optimal fit of the V(R′) curve, and experimentally using the D–L correlation method.

	L_{max} (μm)	
E (MeV)	using (T-T) Track-Test program	using D-L correlation (present method)
5.3	20.76	21.10
4.7	18.55	18.46
4.1	15.99	15.81
3.5	13.14	13.11
	For all used etching temperatures (60, 70, 80 °C)	

D-L: Track Diameter-Length calibration curve based on the track's diameter measurements.
T-T: Track-Test program based on the new estimated coefficients of the V function.

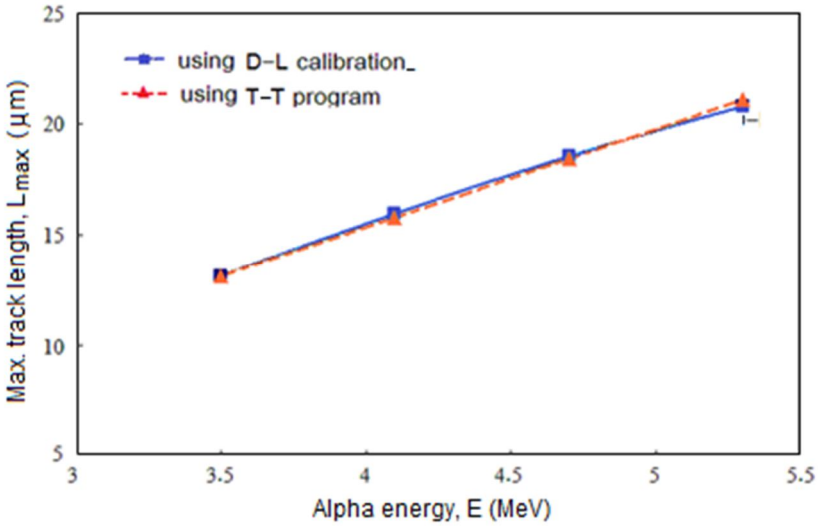

FIG. 16. Comparison of maximum track lengths in CR-39 for alpha energies at all etching temperatures, calculated theoretically using the Track-Test software using the new coefficients obtained from the optimal fit curve of V(R′), and experimentally using the D-L correlation method.

Figure 17 illustrates a comparison between the theoretical and experimental track diameters of 4.7 MeV alpha particles in CR-39 at an etching temperature of 70 °C. The theoretical diameters, calculated using the Track-Test program with the optimal fitting coefficients of the V equation derived from the D–L correlation method, show excellent agreement with the experimentally measured diameters for the same alpha-particle energy and etching conditions.

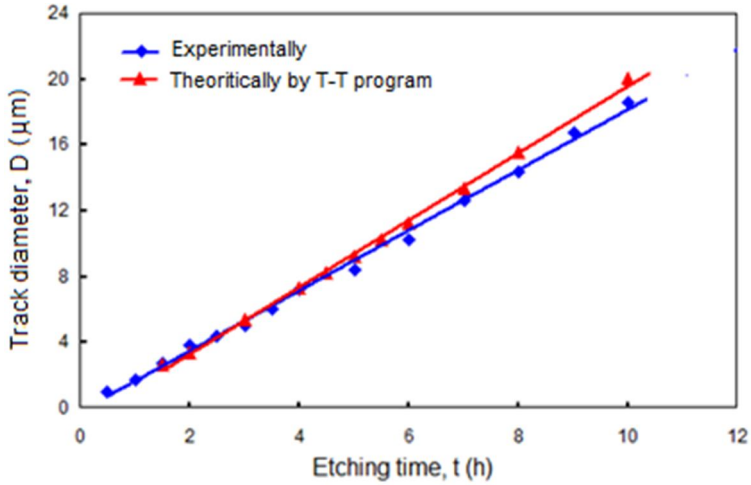

FIG. 17. Comparison of empirical diameters of 4.7 MeV alpha tracks in CR-39 at an etching temperature of 70 °C. The theoretical diameters were calculated using the Track-Test software with the new optimal fitting coefficients derived from the track D–L correlation method.

4. Conclusion

The alternative "D-L correlation" method, which relies on directly measured track diameters in CR-39, successfully determined track profiles and parameters that are in good agreement with results obtained by studies relying on direct measurements of track lengths from etched track images.

The track length curves for different alpha-particle energies display bundle-like patterns corresponding to changes in the etching temperature. While increasing the etching temperature does not affect the maximum track length (L_{max}) at saturation, it reduces the time (T_{sat}) required to reach this maximum. Conversely, for a constant etching temperature, both Lmax and tsat increase with decreasing alpha-particle energy, reflecting the higher energy deposition in the detector material.

It was proved that the evolution of the track profile is greatly influenced by the change of

the track etching rate with its depth, $V_T(x)$. Based on direct measurements of track diameters, the present method yields depth-dependent values of V_T for a given incident particle energy, which represents a key advantage of this approach. This behavior contrasts with earlier studies that relied on direct diameter measurements but assumed a single constant value of V_T with track depth for a single specified energy of the incident particles and used the elementary equations generated for this case, which were unable to accurately predict the real changes in track parameters and shapes.

Finally, the D-L correlation method is easy to use and doesn't require a lot of skill or effort. It shows realistic changes in the track profiles and parameters that are comparable to those obtained by directly measuring the lengths of the tracks from their experimental photos. As a result, this methodology is an alternative to the method of direct measurement of the track length, which requires an appropriate technique, accuracy, and experience in obtaining experimental images of track profiles in the detector.

References

[1] Durrani, S.A. and Bull, R.K., "Solid State Nuclear Track Detection", (Pergamon Press, Oxford, UK, 1987).

[2] Sinenian, N., Rosenberg, M.J., Manuel, M., McDuffee, S.C., Casey, D.T., Zylstra, A.B., Rinderknecht, H.G., Gatu Johnson, M., Seguin, F.H., Frenje, J.A., Li, C.K., and Petrasso, R.D., Rev. Sci. Instrum., 82 (2011) 1.

[3] Thomas, H.S.P., Deas, R.M., Kirkham, L.N., Dodd, P.M., Zemaityte, E., Hillier, A.D., and Neely, D., Plasma Phys. Control. Fusion, 63 (2021) 124001.

[4] Khan, A., Al Qahtani, S., Al-Maqbool, W., Al-Naggar, T.I., Alhamami, A., and Abdalla, A.M., Radiat. Phys. Chem., 213 (2023) 111237.

[5] Dörschel, B., Hermsdorf, D., Kadner, K., and Kühne, H., Radiat. Prot. Dosimetry, 78 (3) (1998) 205.

[6] Hermsdorf, D. and Hunger, M., Radiat. Meas., 44 (9-10) (2009) 766.

[7] Azooz, A.A., Al-Nia'emi, S.H., and Al-Jubbori, M.A., Radiat. Meas., 47 (2012) 67.

[8] Yu, K.N., Ng, F.M.F., and Nikezic, D., Radiat. Meas., 40 (2005) 380.

[9] Yu, K.N., Ng, F.M.F., Ho, J.P.Y., Yip, C.W.Y., and Nikezic, D., Radiat. Prot. Dosimetry, 111 (1) (2004) 93.

[10] Ng, F.M.F., Luk, K.Y., Nikezic, D., and Yu, K.N., Nucl. Instrum. Methods Phys. Res. B, 263 (2007) 266.

[11] Wertheim, D., Gillmore, G., Brown, L., and Petford, N., Nat. Hazards Earth Syst. Sci., 10 (2010) 1033.

[12] Nikezic, D., and Yu, K.N., Radiat. Meas., 37 (2003) 39.

[13] Dörschel, B., Hermsdorf, D., Reichelt, U., Starke, S., and Wang, Y., Radiat. Meas., 37 (2003) 563.

[14] Tse, K.C.C., Nikezic, D., and Yu, K.N., Radiat. Meas., 43 (2008) 98.

[15] Dörschel, B., Fülle, D., Harmann, H., Hermsdorf, D., Kadner, L., and Radlach, CH., Radiat. Prot. Dosimetry, 69 (4) (1997) 267.

[16] Azooz, A.A., Al-Nia'emi, S.H., and Al-Jubbori, M.A., Comput. Phys. Commun., 183 (2012) 2470.

[17] Al-Nia'emi, S.H.S., Iraqi J. Sci., 59 (2B) (2018) 856.

[18] Al-Nia'emi, S.H.S., J. Phys. Sci., 29 (2) (2018) 89.

[19] Nikezic, D. and Yu, K.N., Comput. Phys. Commun., 178 (2008) 591.

[20] Nikezic, D. and Yu, K.N., Comput. Phys. Commun., 174 (2006) 160.

[21] Nikezic, D., Ivanovic, M., and Yu, K.N., Softw. X, 5 (2016) 74.

[22] Younes, O.K., MSc. Thesis, Department of Physics, College of Education for Pure Scince, University of Tikrit, (2016).

[23] Ziegler, J.F., Ziegler, M.D., and Biersack, J.P., The stopping and range of ions in matter,

SRIM-2008, (2008), http://www.srim.org.

[24] Green, P.G., Ramli, A.G., Al-Najjar, S.A.R., Abu-Jarad, F., and Durrani, S.A., Nucl. Instrum. Methods, 203 (1982) 551.

[25] Saeed, S.H. and Mustafa, A.Q., Kirkuk Univ. J. Sci. Stud., 16 (3) (2021) 12.

[26] Ditlov, V.A., Awad, E.M., Fromm, M., and Hermsdorf, D., Radiat. Meas., 40 (2005) 249.

[27] Yamauchi, T., Ichijo, H., Oda, K., Dörschel, B., Hermsdorf, D., Kadner, K., Vaginay, F., and Fromm, M., Radiat. Meas., 34 (2001) 37.

[28] Brun, C., Fromm, M., Jouffroy, M., Meyer, P., Groetz, J.E., Abel, F., Chanbaudet, A., Dörschel, B., Hermsdorf, D., Bertschneider, R., Kadner, K., and Kuhne, H., Radiat. Meas., 31 (1999) 89.

[29] Fromm, M., Awad, M., and Ditlov, V., Nucl. Instrum. Methods Phys. Res. B, 226 (2004) 565.

[30] Nikezic, D. and Yu, K.N., Mater. Sci. Eng. R, 46 (2004) 51.